ICES Journal of Marine Science

ICES Journal of Marine Science (2018), 75(3), 1131–1142. doi:10.1093/icesjms/fsx204

Original Article

Broadband echosounder measurements of the frequency response of fishes and euphausiids in the Gulf of Alaska

Christopher Bassett*, Alex De Robertis, and Christopher D. Wilson

Alaska Fisheries Science Center, National Marine Fisheries Service, National Oceanic and Atmospheric Administration, 7600 Sand Point Way NE, Seattle, WA 98115, USA

**Corresponding author: tel: +1 (206) 526-4682; fax: +1 (206) 526-6723; e-mail: chris.bassett@noaa.gov*

Bassett, C., De Robertis, A., and Wilson, C. D. 2017. Broadband echosounder measurements of the frequency response of fishes and euphausiids in the Gulf of Alaska. – ICES Journal of Marine Science, 75: 1131–1142.

Received 30 May 2017; revised 2 October 2017; accepted 8 October 2017; advance access publication 13 November 2017.

Broadband acoustic scattering techniques are not widely used in fisheries acoustics, but this may change due to the recent commercial availability of a broadband echosounder system operating at frequencies commonly used in fisheries surveys. A four-channel (15–150 kHz) broadband echosounder was used to investigate the potential of broadband methods to improve species discrimination during a walleye pollock (*Gadus chalcogrammus*) survey in the Gulf of Alaska. Narrowband echosounders combined with mid-water and bottom trawls were used to identify aggregations of interest for broadband measurements. Broadband frequency responses were measured for multiple pelagic and semi-demersal fishes as well as euphausiids. No clear patterns in the broadband frequency responses were identified that would aid in discrimination among the commonly encountered swimbladder-bearing species. The results are consistent with narrowband observations and suggest that both techniques face the same challenges when attempting to discriminate among acoustically similar species as frequency responses overlap within the measured bandwidth. However, examples are presented in which broadband frequency responses provide additional information about near-resonant scatterers. The benefits of broadband operations have not been fully realized and widespread adoption of broadband techniques and improved processing algorithms may yield improved acoustic-based species discrimination for use during fisheries surveys.

Keywords: broadband acoustic backscattering, Simrad EK80 echosounder, species discrimination.

Introduction

Acoustic-trawl (AT) surveys support fisheries management by combining remote sensing and physical sampling techniques to provide abundance estimates. Acoustic methods allow for relatively rapid sampling of large volumes of water, but are limited in their ability to discriminate among species (Horne, 2000). In AT surveys, species compositions and length-frequency distributions from occasional midwater and bottom trawls are combined with acoustic backscatter data from one or more narrowband echosounders to attribute backscatter to different species and size classes (Greenlaw, 1979; McClatchie *et al.*, 2000; Jech and Michaels, 2006). Direct sampling methods (e.g. trawl hauls), however, are time consuming allowing for only a limited number of trawls on a given survey. In addition, the size and species composition of the catch may not reflect that of the organisms in the environment (Wileman *et al.*, 1996; Williams *et al.*, 2011). Thus, target identification is a major source of uncertainty and any additional information that can be derived from acoustic backscatter could increase efficiency and reduce biases in AT surveys.

It is well-known that multiple frequencies can be used to distinguish among acoustically diverse groups (e.g. swimbladder-bearing fish vs. euphausiids), but that discrimination amongst acoustically similar species or age classes of a single species is difficult (Horne, 2000; De Robertis *et al.*, 2010). Broadband acoustic backscatter systems differ from narrowband systems, which transmit a pulsed wave of a single frequency, in that they typically transmit a frequency-modulated signal that may span up to an octave or more. Broadband systems offer additional information in the form of a continuous measurement of frequency-dependent backscatter within the measurement band. They are

becoming more prevalent in fisheries research and there is an interest in exploiting their additional capabilities. For example, it may be possible to use broadband acoustic measurements to better discriminate among species by using the additional bandwidth to identify acoustic features associated with distinctive morphological characteristics or size (Lavery *et al.*, 2007; Stanton *et al.*, 2010).

Early studies of broadband biological reverberation in the marine environment (Chapman and Marshall, 1966; Holliday, 1972) relied on explosives as sound sources, but unreliable source levels and low duty-cycles limited their widespread adoption. More recent use of broadband systems with better controlled source levels both *in situ* (Simmonds and Armstrong, 1990; Zakharia *et al.*, 1996; Lavery *et al.*, 2010; Stanton *et al.*, 2010; Ross *et al.*, 2013) and in laboratories (Chu and Stanton, 1998; Stanton *et al.*, 1998) has demonstrated the potential of broadband systems for discriminating not only among biological scatterers, but also physical sources of scattering [e.g., turbulent mixing, microstructure (Lavery *et al.*, 2010, 2013)]. Although broadband systems have been commercially available, if not widely adopted, for more than a decade (Ehrenberg and Torkelson, 2000), these studies were historically performed using custom systems. The recent commercial release of broadband echosounder systems similar to those used widely in fisheries acoustics (e.g. the Kongsberg Simrad EK80), and the availability of existing wide-bandwidth transducers on many research vessels have generated further interest in the adoption of broadband techniques in fisheries surveys.

Broadband signals and pulse compression processing techniques, often referred to as matched-filter processing (Turin, 1960), have been applied extensively in other fields including radar (Westerfield *et al.*, 1960), acoustic flaw detection in materials (Papadakis and Fowler, 1969), and sub-bottom profiling (Henkart, 2006). In contrast to narrowband signals, broadband signals can be processed to improve the signal-to-noise ratio and temporal/range resolution (Chu and Stanton, 1998; Ehrenberg and Torkelson, 2000; Stanton, 2012). Although the improved range resolution and higher signal-to-noise ratios are widely exploited in other applications, the potential for better target characterization using the frequency response (i.e. frequency spectrum) has not been widely investigated. The broadband approach differs from narrowband techniques primarily in that the volume backscatter spectrum can be analysed over a wider bandwidth with fine frequency resolution. An important research question is the degree to which taxonomic discrimination techniques can be improved by characterizing the nearly continuous frequency spectra, as opposed to the limited number of discrete frequencies available from multi-frequency narrowband systems.

Surveys using narrowband echosounders regularly attempt to discriminate among taxa in near real-time to support human interpretation of the observations and the decision to trawl in a given location. This is often accomplished by comparing observations of frequency response to statistics compiled from the measured or modelled frequency-dependence of taxa-specific backscatter (SIMFAMI, 2005; Fernandes, 2009; De Robertis *et al.*, 2010; Ressler *et al.*, 2012; Woillez *et al.*, 2012; Korneliussen *et al.*, 2016). The principle underlying this approach is that the physical characteristics of animals such as size or anatomical features (e.g. a swimbladder or other gas inclusion) result in distinct frequency-dependent scattering that, when coupled with *a priori* knowledge of the likelihood of a species being present, can be used to identify the sound-scattering organisms. Although organisms with large differences in frequency-dependent scattering can be readily distinguished from dissimilar scatterers (Ressler *et al.*, 2012), it is much more difficult to discriminate among animals that are characterized by more subtle differences in frequency response. The extent to which the increased bandwidth and frequency resolution afforded by broadband systems can be leveraged to improve species discrimination based on these differences remains an open question.

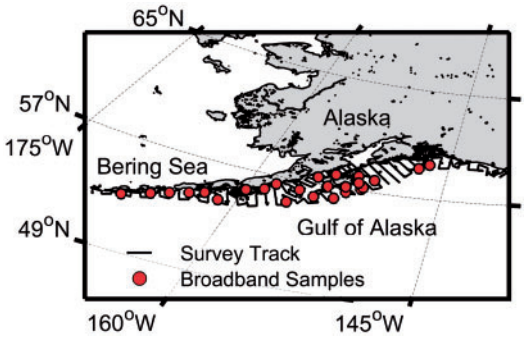

Figure 1. Ship tracklines and broadband sample locations for the summer 2015 Gulf of Alaska walleye pollock survey.

To address the utility of broadband measurements for species discrimination during fisheries surveys, this study focuses on the mean frequency response of aggregations given its widespread use as a method for target characterization. Measurements from four broadband channels (15–150 kHz with gaps) obtained during a walleye pollock survey in the Gulf of Alaska are reported. The objectives of the work are to (i) calibrate the system and adapt existing post-processing methods to establish a broadband frequency response, (ii) characterize the broadband frequency response of the species encountered during the survey, and (iii) compare the results to historical narrowband measurements of frequency response.

Methods

Broadband backscatter measurements of the species encountered during an AT survey in the Gulf of Alaska were made between 10 June and 8 August 2015 (Figure 1). The approach was to opportunistically conduct dedicated broadband measurements in areas where aggregations of species of interest were identified during routine survey operations, thereby evaluating the potential advantages of measuring the broadband frequency responses in a survey context. The following sections include a description of the broadband acoustic system, calibration and post-processing information, as well as a summary of how sampling sites were selected during the survey, and how the biological scattering sources in these aggregations were identified. The signal processing procedures used in this study are the same as those applied by Simrad (Demer *et al.*, 2017) and are similar to those described elsewhere (Jech *et al.*, 2017; Lavery *et al.*, 2017).

Broadband echosounder system

The broadband echosounder system employed consisted of four Simrad EK80 wide band transceivers (WBTs) driven by a desktop computer (EK80 software version 1.8.0) and four Simrad split-beam transducers (nominal frequencies: 18, 38, 70, and 120 kHz) mounted on the ship's centreboard. The signals received on each of the four channels of the split-beam echosounders are digitized at 1.5 MHz and are filtered and decimated (i.e. the sampling rate

reduced) in two stages. First, echoes are passed through a hardware filter and decimated. A second-stage software filter, followed by additional decimation, results in the final, complex-valued data that are saved for post-processing (Demer *et al.*, 2017). The software filter and final decimation factor are determined by the software based on the transmit signal's parameters. Storing the decimated data prior to pulse compression significantly reduces the data rate, while allowing for flexibility in post-processing (i.e. a broader range of post-processing techniques can be applied compared with storing data after pulse compression). Each file includes metadata about the transmit signals, filters, and decimation factors that are required for post-processing of the received echoes. All post-processing was performed using custom MATLAB scripts. Table 1 includes details about the four transducers, transmitted signals, final sampling rates, and other beam parameters.

Transmitted signals

The EK80 software permits the generation and transmission of linear frequency-modulated signals, referred to as chirps, over a restricted set of user-specified frequencies that overlap with the transducer's specified nominal frequency. The analysed frequency ranges for the four transducers were 15–25, 35–38, 50–87, and 100–150 kHz, respectively. The EK80 software offered two transmit signals tapers—"fast" and "slow". A "fast" taper, which was used for the 18, 70, and 120 kHz transducers, applies a half-raised cosine taper to the beginning and end of the signal. The "slow" taper applies a Hann (raised-cosine) window to the entire transmit signal and was used on the 38 kHz channel due to hardware and software limitations. Additional information about these signals and their impact is described elsewhere (Chu and Stanton, 1998; Demer *et al.*, 2017; Lavery *et al.*, 2017). Due to the taper and increased noise levels later attributed to a damaged transducer cable, the 38 kHz data exhibited low signal-to-noise ratios and the useful bandwidth obtained with the transducer was limited to a narrow band near the transducer's nominal frequency.

Calibration

The broadband system was calibrated *in situ* on 11–12 June 2015, using three calibration spheres: a 64-mm diameter copper sphere and 25- and 38.1-mm diameter tungsten-carbide (WC) spheres with a 6% cobalt binder. The acoustic properties of the spheres were assumed to match those reported in Foote and MacLennan (1984). A Sea-Bird (SBE-911plus) conductivity, temperature, and depth sensor deployed at the calibration site was used to calculate the water sound speed, $c_w = 1478.4\ \mathrm{m\,s^{-1}}$, at the depth of the sphere (Francois and Garrison, 1982a, b).

The broadband frequency response for a given calibration sphere, depending on the transmitted bandwidth and target size, may contain nulls that complicate calibration procedures (Dragonette *et al.*, 1981; Foote, 2000; Atkins *et al.*, 2008; Stanton, 2012; Hobæk and Forland, 2013; Lavery *et al.*, 2017). As a result, multiple calibration spheres with different sizes and material properties can be used to account for the frequency response across the transmitted bandwidth using portions of the theoretical target strength curve that are relatively well-behaved (i.e. portions of the curve with few nulls). This approach minimizes the need for interpolation. Combining results obtained with different spheres should produce smooth calibration curves with no offsets or other artefacts derived from the different targets across the bandwidth of the transducer.

Table 1. Transducer and analysis parameters.

Transducer	ES18-11	ES38B	ES70-7C	ES120-7C
Nominal frequency (kHz)	18	38	70	120
Transmit frequency range (kHz)	12–28[a]	30–42[a]	47–90	95–155
Analysis frequency range (kHz)	15–25	35–38	50–87	100–150
Transmit signal duration (ms)	2.048	2.048	4.096	4.096
Transmit power (W)	2000	2000	1000	250
f_{dec} (kHz)	23.438	15.625	62.500	125.000
Beamwidth at f_{nom} (°)	11	7	7	7
$10\log_{10}(\Psi_{nom})$	−17.4	−20.7	−21.0	−21.3
Range resolution, $\frac{1}{2}\frac{c_w}{B}$ (cm)	7.4	24.6	2.0	1.5
N_{FFT}	48	32	128	256

The sampling rate for all frequencies prior to filtering and decimation is 1.5 MHz and the post-decimation sampling rate is f_{dec}. The range resolution is calculated using a sound speed of 1478 m s^{-1} and the analysis bandwidth. N_{FFT} is the number of data points used in the Fast Fourier Transform of the compressed pulse output and corresponds to the window length closest to 1.5 m. The resulting frequency resolution is 488 Hz.

[a]Simrad does not recommend broadband operation of these transducers. Although the ES18-11 provided acceptable broadband results, measurements from the ES38B were limited to frequencies near the specified nominal frequency.

The basic calibration procedures for broadband echosounders otherwise follow those used to calibrate narrowband systems (Demer *et al.*, 2015). Use of the 38.1- and 25-mm WC targets yielded similar calibration curves (the response of the 64 Cu sphere is too complicated for effective use at high frequencies), suggesting that a linear interpolation of the 38.1-mm WC response across the nulls was a good approximation. Despite the similarities, a small (<0.5 dB) but systematic offset between the 25- and 38.1-mm WC spheres was consistently observed. The source of this discrepancy, which has been reported by others (Hobæk and Forland, 2013), was not identified. Because this study focuses primarily on comparing the spectral structure as opposed to the amplitude of the volume backscatter curves, this offset was not critical for this application so long as the same calibration curve was used in all cases. Therefore, calibration results from the 38.1-mm WC sphere were used for all channels.

Calibration curves were initially generated using a custom MATLAB script. Split-beam processing (Simmonds and MacLennan, 2005) of the compressed-pulse data was performed on the calibration echoes to identify the location of the targets within the beam. The split beam processing requires angle sensitivities that depend on frequency and sound speed. These can be independently calculated in controlled experiments or assumed to match nominal manufacturer specifications (Demer *et al.*, 2015). In this case, simultaneous measurements of electrical and mechanical angle at the −3 dB points of the transducers, which were provided by the manufacturer, were used to derive estimates of the angle sensitivity at the nominal frequencies of each transducer. Calibration data were manually reviewed to remove instances where echoes from other targets (e.g. fish) appeared within 2 m of the sphere. Targets <0.2 degrees off-axis (10–20 pings retained per channel) were averaged to produce the calibration curves. At the highest frequencies transmitted by the different transducers, these restrictive off-axis limits require <0.5 dB of compensation for the two-way beam pattern.

After this calibration procedure was implemented, the manufacturer released software with improved single-target detection algorithms for calibration processing. The curves derived using

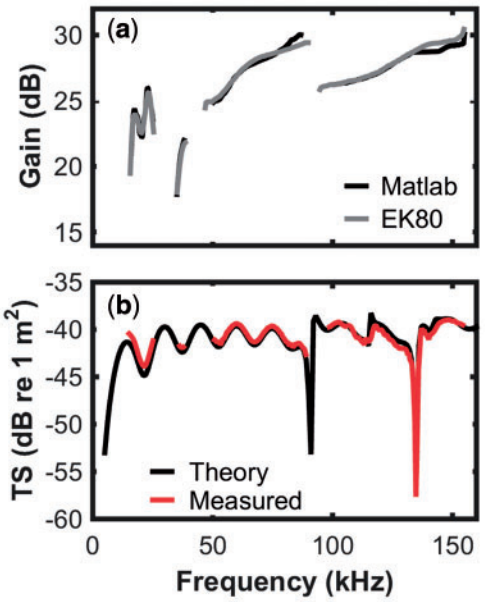

Figure 2. (a) Calibration curves obtained using the EK80 software and the MATLAB script. The curves agree well except near the edges of the bands and near nulls in the theoretical target strength curve for the 38.1-mm WC sphere. (b) A comparison between the theoretical scattering curve for the 38.1-mm WC sphere and the measurements when applying the calibration curve generated by the EK80 software.

the method described earlier are shown in Figure 2 with the calibration results later post-processed using the EK80 software (version 1.8.3) and over 1000 pings per transducer. Calibration curves generated using both methods agree well despite small differences that are attributed to different methods for interpolating across the nulls. Given the agreement between both methods, the calibration curves from the EK80 software were applied in further processing as this method is more likely to be used in future studies. Figure 2b shows good agreement between the theoretical targets strength curve and measurements from the 38.1-mm WC sphere across the analysed bandwidths with the calibration curves applied.

The volume sampled by the beam, which changes as a function of frequency for a fixed-size transducer, must be characterized for calibrated measurements of volume scattering. As with narrowband measurements, the beam volume can be calculated according to theory or by using off-axis targets during calibration if the angle sensitivities are known. Both approaches were compared to ensure the system was operating as expected. By moving the target throughout the beam and plotting the normalized amplitude vs. the target location within the beam the combined transmit and receive beam pattern is obtained at each frequency. Here the beam patterns were assumed to be axisymmetric, and no significant deviations from this assumption were noted. The combined beam pattern at each frequency is fit with a third order polynomial and compared with the theoretical beam pattern for a piston transducer (Medwin and Clay, 1998; Simmonds and MacLennan, 2005). Figure 3a illustrates good agreement between the measured beam pattern for the 47–90 kHz channel at 70 kHz, the theoretical beam pattern given the transducer's beamwidth at the nominal frequency, and a third-order polynomial fit to the

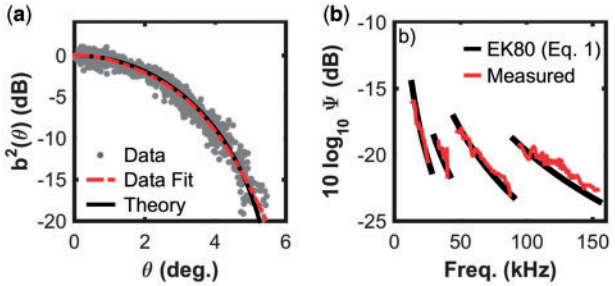

Figure 3. (a) Comparison of the observed squared (i.e. two-way) beam pattern at 70 kHz, the theoretical two-way beam pattern given the transducer's specifications, and a third order polynomial fit to the data. (b) The equivalent beam angle vs. frequency based on the transducer's specifications combined with Equation (1), and the equivalent beam angle calculated by integrating the fits to the data.

observations. Equivalent beam angles (ψ) were calculated by integrating the empirical fits to the main-lobe as a function of frequency (Simmonds and MacLennan, 2005). These results are compared with the relationship used by Simrad,

$$\Psi(f) = \Psi_{f_{\mathrm{nom}}} - 20\ \log_{10}\left(\frac{f}{f_{\mathrm{nom}}}\right), \qquad (1)$$

where f_{nom} is the nominal frequency of the transducer and $\Psi_{f_{\mathrm{nom}}}$ is the equivalent beam angle of the transducer at f_{nom}. This term accounts for the theoretical decrease in beamwidth with increasing frequency for a fixed-size transducer (Medwin and Clay, 1998). Figure 3b shows the good agreement between $\Psi(f)$ calculated from the measurements and according to Equation (1), which is the form used in calculations of volume backscatter.

Broadband acoustic measurements

The broadband measurements were collected periodically during a large-scale walleye pollock AT survey of the Gulf of Alaska (Jones *et al.*, 2017). The survey uses narrowband acoustic measurements and trawl catches to attribute the acoustic backscatter to unique taxa and age classes. The narrowband measurements (i.e. Simrad EK60 at 18, 38, 70, 120, and 200 kHz) were collected throughout the survey. Trawl hauls targeting aggregations of fishes were conducted using either a pelagic Aleutian Wing Trawl (AWT) (Guttormsen *et al.*, 2010) or a Poly-Nor'Eastern bottom trawl (Stauffer, 2004). Trawl haul depths and mouth openings were measured using either a Simrad FS70 or a Furuno CN24 trawl monitoring system. The AWT was fitted with a stereo camera system mounted in the aft region of the trawl to determine whether species were stratified by depth when the catch composition was not dominated by a single species (Williams *et al.*, 2010). In addition, nine Methot trawl hauls (Methot, 1986) were conducted during the survey to verify the species composition of suspected euphausiid aggregations.

These tools were used to identify aggregations dominated by a single species or taxon for broadband acoustic backscatter measurements. Assignment of the backscatter to a species was based on the species composition of the trawl catch for most fishes. Backscatter was attributed to euphausiids or mesopelagic fishes by applying narrowband multi-frequency algorithms based on historical measurements in the same geographic region (De Robertis *et al.*, 2010). To collect broadband measurements

with the same transducers as the narrowband survey, the transducer cables were disconnected from the EK60 transceivers and connected to the WBT corresponding to the same nominal frequency. The broadband measurements on the same aggregation(s) were collected over periods of 12–70 min with a 1 Hz sampling rate and synchronous pings [Calibration was also performed using synchronized pinging. More recent work (Demer *et al.*, 2017) suggests the potential for crosstalk between channels in this configuration and advises against synchronous pinging until the issue is further studied. Calibration should be performed using the same configuration as data collection.]. The distance covered by these broadband measurements was based on the size of the aggregations of interest, but it always exceeded the spatial extent of the targeted aggregations. It was assumed that the species composition did not change between narrowband and broadband measurements.

Broadband measurements chosen for further analysis were selected to maximize the number of observations of different single-species aggregations commonly encountered in the survey area. Volume backscatter spectra, S_v, were produced for an aggregation by first identifying pings and depths that had relatively constant levels of S_v in the temporal domain. For each set of pings and depth ranges containing the data of interest, the centre of a new data window was taken every 0.25 m. The individual data windows were processed and averaged in linear units to produce a representative S_v spectrum for the aggregation. With a window length of 1.5 and 0.25 m separation there was an 83% overlap between windows. This overlap resulted in a smoother spectrum, but means that samples used to produce the average were not statistically independent. The volume represented by each ping at the nominal frequency was dependent on the depth and thickness of the aggregations but ranged from 60 to >4000 m^3. Combining the depth ranges and number of pings with a typical vessel speed of 6 knots (3.1 $m\,s^{-1}$), the approximate sampled volumes for the aggregations ranged from 180 m^3 for relatively shallow (~50-m depth), small schools of pollock to >29 000 m^3 for deeper (~300-m depth) mesopelagic layers. Over 80% of the sampled aggregations, as processed, had volumes between 200 and 3000 m^3.

Calculation of broadband frequency responses

The number of data points processed to produce frequency spectra can be dictated in post-processing based on the desired application (e.g. target strength vs. volume backscatter) or desired frequency resolution. Using a longer portion of the time series (hereafter, window length), increases the frequency resolution of the spectrum. However, if the window length is longer than the matched-filter response for the target of interest, or if another target is present within the window, the spectrum will be affected by this additional noise. Therefore, the desired window length balances the need to have enough data to observe structure in the frequency response vs. limiting the window length to effectively characterize single targets. Here, all data are presented using 1 ms (~1.5 m) data windows, which results in a frequency resolution of 488 Hz. Backscatter from the targeted aggregations was sufficiently dense that individual targets were indistinguishable and windows included multiple targets.

Given that aggregation behaviour changes with density and environmental cues such as time of day, discrimination among taxa based on S_v values alone is a poor choice as this depends on numerical abundance as well as the acoustic properties of the animals present. Thus, a s_v (linear units) ratio, or relative frequency response, approach is commonly used as this does not depend on numerical density (SIMFAMI, 2005; Korneliussen *et al.*, 2009, 2016; De Robertis *et al.*, 2010). This presentation preserves the spectral shape, which is driven by factors related to the physiology and behaviour of a species while removing any amplitude offsets driven by the density of animals within an aggregation.

To replicate this approach for broadband data, a representative spectrum for each species is calculated. An S_v curve is initially obtained by taking the $\log_{10}$ of the average of the raw s_v spectra for the aggregation. This average is then normalized by $\overline{S_v}$ $(114-126\ \text{kHz})$, which is the mean value (log space) of the spectrum from 114 to 126 kHz. The relative frequency response, in decibels, of an aggregation, ΔS_v, is then described by $\Delta S_v(f) = S_v(f) - \overline{S_v}(114-126\ \text{kHz})$. Backscatter observations are often normalized by the amplitude at 38 kHz in fisheries work (Korneliussen and Ona, 2003; De Robertis *et al.*, 2010). However, the 120 kHz channel was used in this case because of concerns with the data quality of the 38 kHz channel. An average curve for the species, $\langle \Delta S_v \rangle$, is created by averaging all ΔS_v curves from the individual aggregations for that species. These results are compared directly to narrowband frequency-differences for the same species established from previous surveys in the area (De Robertis *et al.*, 2010). Slopes are calculated for the ΔS_v curves by performing a linear, least-squares regression on the data, excluding the 38 kHz channel.

Catch composition and broadband acoustic samples

Twenty-eight broadband acoustic samples were obtained. Trawl-hauls were analysed for species composition and length-frequency distributions of the dominant species. Aggregations not dominated (>95% by weight and number) by a single species based on trawl data were excluded from further analysis (see below for two exceptions). Thus, subsequent analyses included aggregations dominated by either walleye pollock (*Gadus chalcogrammus*), Pacific ocean perch (*Sebastes alutus*), Pacific herring (*Clupea pallasii*), euphausiids (typically *Thysanoessa inermis* in areas west of Prince William Sound; Simonsen *et al.*, 2016), or mesopelagic fishes. Two mixed species aggregations were also included: (i) capelin (*Mallotus villosus*) and Pacific herring and (ii) northern rockfish (*Sebastes polyspinis*) and Pacific cod (*Gadus macrocephalus*).

Results

Catch composition

Twenty-one of the 28 broadband samples were identified for further analysis based on species composition thresholds and the presence of well-defined, separable aggregations from which S_v curves could be determined. Some of these samples included aggregations of multiple spatially separated taxa (e.g. walleye pollock and euphausiid aggregations). The total number of observations analysed for the different taxa is summarized in Table 2. At least one well-defined aggregation was manually identified and used to construct independent S_v curves for each of the sampled taxa.

The fishes dominating the trawl hauls in the locations where broadband measurements were conducted exhibited mainly unimodal size distributions and in some cases bi-modal size distributions (a figure showing the length-frequency distributions of fishes captured in the trawl-hauls is available as online

Table 2. Number of broadband acoustic samples and aggregations classified by taxonomic group based on catch composition and/or EK60 observations.

Species	Number of hauls	Aggregations analysed
Walleye pollock	12	24
Pacific ocean perch	4	7
Pacific herring	1	7
Capelin and Pacific herring (mixture)	1	1
Northern rockfish and Pacific cod (mixture)	1	2
Mesopelagic fishes	–	2
Euphausiids	–	11

Supplementary Material). Walleye pollock aggregations were composed of either a single size class (30–42 cm) or a bimodal distribution also including fish between 20 and 30 cm. Small numbers of fish larger than 42 cm were present in all trawl hauls. Pacific ocean perch aggregations were dominated by fish between 25 and 40 cm in length. Trawl camera observations from a mixed aggregation of capelin and Pacific herring showed that the two species were mixed in a diffuse layer. Capelin comprised ~80% of the catch (by number) vs. 20% for herring. Both species had similar length distributions (8–13 cm). The other mixed aggregation data were from a bottom-trawl that was dominated by northern rockfish (87% by number) although Pacific cod (9%), flatfishes (<3%), and other rockfishes (<1%) were also present. Mean euphausiid lengths and standard deviations from the nine Methot trawls were 19.3 ± 1.9 mm with euphausiids comprising 96% of the catch by number, which is consistent with previous observations on this survey (Simonsen *et al.*, 2016).

Observations of frequency response

Raw S_v spectra (i.e. those derived from a single data window) exhibit high ping-to-ping variability. These variations are driven by many factors including the density of animals, random motion and orientation changes between pings, and frequency-dependent backscatter from animals. Thus, the resulting spectra can be smooth, well-structured (e.g. regularly space peaks and nulls), or highly variable. Figure 4 shows an echogram of a euphausiid aggregation, an S_v spectrum for a single ping, the envelope encompassing 95% of the individual S_v spectra, and the average S_v spectrum for a portion of the aggregation. The raw spectra show that individual windows deviate by over 20 dB from the mean. Although the variability observed from individual windows may contain useful information for species classification, this has not been well-established, and is beyond the scope of this work.

Averaging is necessary to reduce variability, produce a smooth S_v curve, and develop statistical descriptions of S_v spectra that can be applied in species discrimination algorithms. This is illustrated in Figure 5, which includes probability density functions (PDFs) and statistics derived from 1.5-m windows on single-species aggregations of walleye pollock, Pacific herring, and Pacific ocean perch, which all possess swimbladders. The ΔS_v distributions calculated for a single frequency bin (70 kHz) have standard deviations >5 dB. When averaging over multiple frequency bins (66.5–73.5 kHz) the distributions of $\overline{\Delta S_v}$ are considerably narrower and have standard deviations <2.5 dB for all three aggregations. The mean slopes of ΔS_v for all three aggregations are between −1.7 and −2.4 dB per 100 kHz. Fits to the ΔS_v curve for individual pings within all three

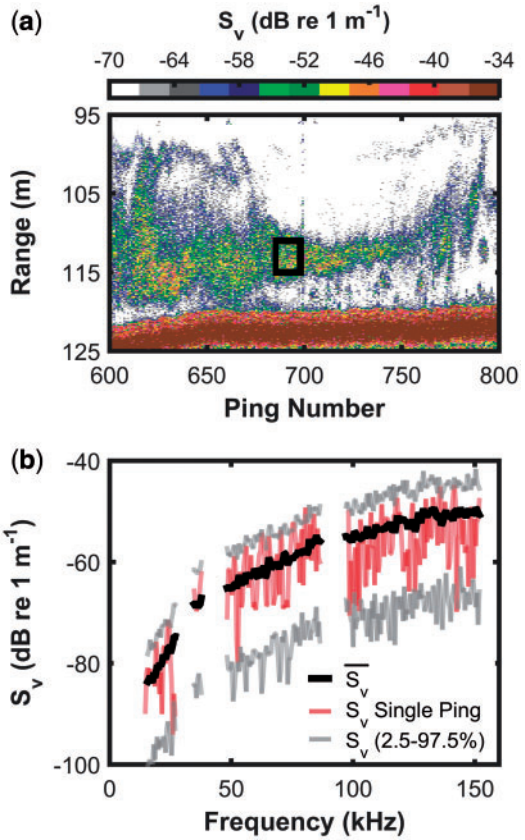

Figure 4. (a) Echogram from the 120 kHz channel showing a euphausiid aggregation. The black box shows the portion of the aggregation used to calculate the representative S_v spectra in (b). (b) The average spectrum based on 100 windows, the spectrum for a single ping, and the envelope for 95% (2.5–97.5%) of the raw spectra. The individual pings are highly variable, but show a frequency response consistent with that of euphausiids. Only through averaging does the curve become relatively smooth.

aggregations yield slopes from −8 dB per 100 kHz to >2 dB per 100 kHz. All of these examples demonstrate substantial noise inherent in values derived from unaveraged S_v spectra.

Raw ΔS_v and $\langle \Delta S_v \rangle$ spectra for all of the species encountered highlight the challenges in species discrimination among acoustically similar species as well as situations in which the added bandwidth provides clear benefits (Figure 6). Average frequency responses for monospecific aggregations of walleye pollock, Pacific ocean perch, Pacific herring, and a mixture of northern rockfish and Pacific cod have similar structures. The similarities in $\langle \Delta S_v \rangle$, combined with the variability in ΔS_v, again highlight the challenge of using basic metrics for species discrimination. For a single, diffuse layer of capelin and Pacific herring of similar size (8–13 cm) the spectrum has a steeper slope at low-frequencies than the other fishes. The curve representing the average frequency response of euphausiids clearly shows the transition between the Rayleigh and geometric scattering regimes. Two examples of measurements from different layers of mesopelagic fishes from a single broadband sample exhibit different frequency responses with peaks between 20 and 38 kHz. Finally, a curve from an unknown source includes a resonance peak (described in detail below) in the 18 kHz channel. Figure 6 also includes historical narrowband observations of

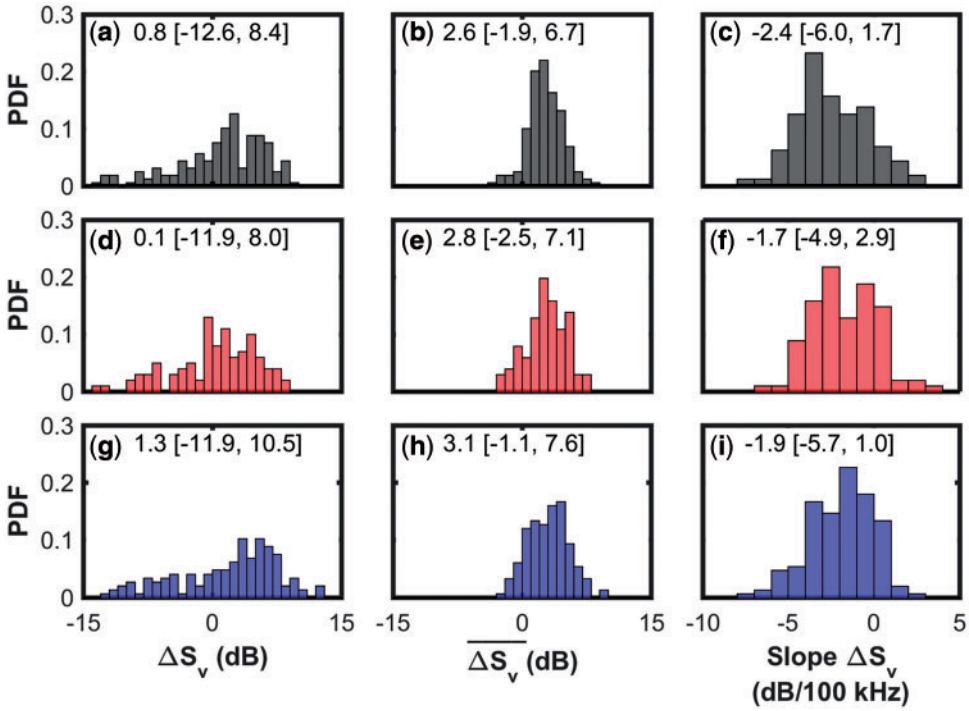

Figure 5. PDFs with 1 dB bins of the multiple statistical quantities derived from individual 1.5-m windows from one single-species aggregation of walleye pollock (n = 140 windows), Pacific herring (n = 102 windows), and Pacific ocean perch (n = 165 windows). Each subplot shows the mean values and ranges for 95% (2.5–97.5%) of the distributions. (Column 1) The ΔS_v at 70 kHz. (Column 2) $\overline{\Delta S_v}$ (averaged from 66.5 to 73.5 kHz; linear space). (Column 3) The slope of ΔS_v per 100 kHz. (a–c) PDFs for a walleye pollock aggregation. (d–f) PDFs for a Pacific herring aggregation. (g–i) PDFs for a Pacific ocean perch aggregation. There is considerable overlap in the distributions, which suggests that species discrimination based on these metrics is difficult. The use of different processing parameters (i.e. window lengths or averaging of spectra) would have an impact on the statistical distributions, but is unlikely to lead to reliable discrimination of these groups due to similarities in the frequency responses and the high variability. Note that statistics from an individual aggregation are not necessarily consistent with averages derived from multiple aggregations of the same species. For example, here the mean slope for walleye pollock is steeper than Pacific ocean perch, a result that is inconsistent with historical observations (De Robertis *et al.*, 2010) and the average calculated from multiple aggregations.

frequency response for the same species and from the same region (De Robertis *et al.*, 2010). Although the sample sizes may be too small to reliably characterize the variability of the broadband frequency response of these species, there is good agreement between the historical data and the broadband observations (mean deviation = 1.1 dB, range = −0.7 to 2.3 dB).

As demonstrated by some of the examples in Figure 6, there are instances where broadband measurements provide additional insight compared with narrowband measurements. This improved capacity is particularly obvious in cases where scatterers produce relatively high amplitude peaks with narrow bandwidths (e.g. resonance). Echograms, ΔS_v, and comparisons to narrowband data are shown in Figure 7 for two examples with strong frequency responses in the 18 kHz channel. The first example (Figure 7a–c) includes a walleye pollock aggregation at 30–100-m depth with elevated levels of scattering relative to other frequencies in the 18 kHz channel outside of the aggregation. This region's frequency response is attributed to a mixture of small, unknown animals with small resonant gas inclusions and fluid-like scatterers (e.g. euphausiids). Modelled scattering curves arbitrarily adjusted to match the amplitude of the ΔS_v curve are included to show their potential contributions. At low frequencies the modelled mixture is dominated by a fit for a bubble at a depth of 75 m with a 1.4 mm equivalent radius (Love, 1978). Although no observations (e.g., net tows) are available to suggest the presence of a high number of young-of-the-year fish, it is worth nothing that this bubble size would be roughly consistent with the swimbladder of a 2.2 cm age-0 walleye pollock (Coyle and Pinchuck, 2002). This is consistent with the size range expected for young-of-the-year pollock during the survey (Dougherty *et al.*, 2007). At higher frequencies the scattering is consistent with the frequency response of euphausiids, which are modelled using the Distorted-Wave Born Approximation applied to a fluid bent cylinder geometry (Stanton, 1989) for an animal length of 19.3 mm, the mean length of euphausiids from Methot trawls. Acoustic properties ($g = 1.017$ and $h = 1.005$) and aspect ratio are based on measurements of euphausiids in the Bering Sea (Smith *et al.*, 2013) and orientation distributions are assumed to be normal with a mean of 0° and a standard deviation of 27°. The clear resonance peak shows how the additional bandwidth afforded by broadband systems can help constrain the possible interpretations of the observations when other information (e.g. physical samples) is not available.

The second example (Figure 7d–f) is from broadband measurements on a number of near-bottom rockfish aggregations. The 18 kHz channel shows relatively high levels of scattering throughout the water column that do not appear in the higher-frequency channels. This region's frequency responses suggests

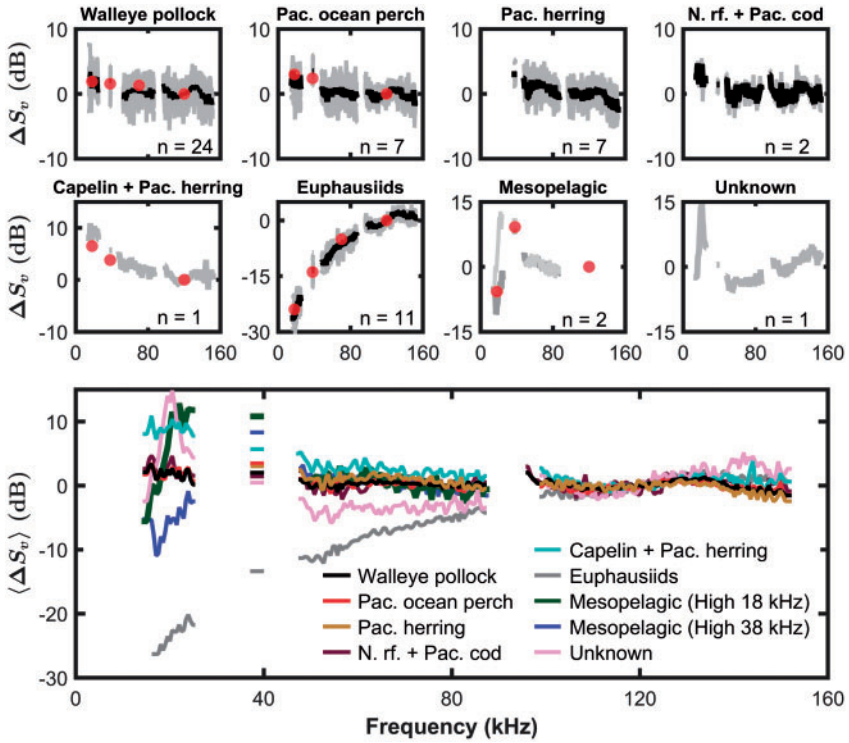

Figure 6. ΔS_v and $\langle \Delta S_v \rangle$ for different single-species aggregations and mixtures encountered during broadband measurements. The small figures include the average curves (black), the curves for the individual aggregations (grey), and the number of individual aggregations (n). The lower inset includes the averages from the upper plots. Two examples are included in the case of mesopelagic fishes due to differences in the frequency response. In the case of the Pacific herring examples, the 18 kHz channel is missing because of a WBT license issue. The dots in some of the subplots highlight historical data using narrowband echosounders for the same species and geographic region (De Robertis *et al.*, 2010).

near-resonance scattering with a peak below 15 kHz, which results in relatively high levels of scattering near 18 kHz but a relatively flat frequency response at higher frequencies. Although narrowband observations also suggests elevated levels of scattering at 18 kHz, the added bandwidth from the broadband measurements confirms that any peak must be below 15 kHz and can, therefore, help constrain the possible interpretations of the observations. The source of this scattering was not retained in the trawl, but concurrent camera observations revealed the presence of small (less than a few centimetres) unidentified fish that may exhibit resonant scattering in this frequency range. Similar elevated levels in broadband 18 kHz echograms relative to the narrowband 18 kHz data channel were noted on multiple transects distributed throughout the survey area.

Discussion

The use of broadband techniques to acoustically discriminate among taxa in the marine environment has been the focus of many studies (Holliday, 1972; Stanton *et al.*, 1998, 2012; Ross *et al.*, 2013; Jech *et al.*, 2017). The additional information associated with the frequency spectra and improved range resolution of pulse compressed data come at the cost of larger datasets along with more complex calibration and processing procedures (Demer *et al.*, 2017; Jech *et al.*, 2017). Despite the additional bandwidth provided by broadband signals, expectations regarding the potential improvements in species discrimination at frequencies commonly used in fisheries surveys (e.g. 18–333 kHz) should be kept in perspective. The principles governing the scattering physics still constrain the available information. As a result, if frequency responses for two species are similar in narrowband observations, significant differences in broadband measurements are unlikely. This, of course, does not mean that broadband scattering measurements cannot improve species discrimination and are an ineffective tool. Rather, expectations for what can be gained through the use of broadband measurements should reflect the challenges of working with complex and highly variable biological scattering sources.

The potential benefits are dependent on the targeted ecosystems and species. Broadband frequency responses were calculated for aggregations of walleye pollock, Pacific ocean perch, Pacific herring, capelin, euphausiids, unknown mesopelagic fishes, and unidentified scatterers encountered in the Gulf of Alaska. Analysis of frequency responses from these aggregations suggests that the additional spectral information does not provide obvious advantages when applying frequency differencing methods to dominant taxa targeted during this survey (i.e. large fishes with swimbladders cannot be distinguished), but they may be helpful for characterizing smaller fishes with swimbladders near resonance. Of course, these results are based on small sample sizes and relatively simple algorithms. Thus, the development of other discrimination algorithms (e.g. those that rely on other metrics besides the mean frequency response) that could perform better than narrowband approaches may be possible.

Random differences in the volume backscatter from ping-to-ping result in noisy S_v spectra computed from small volumes.

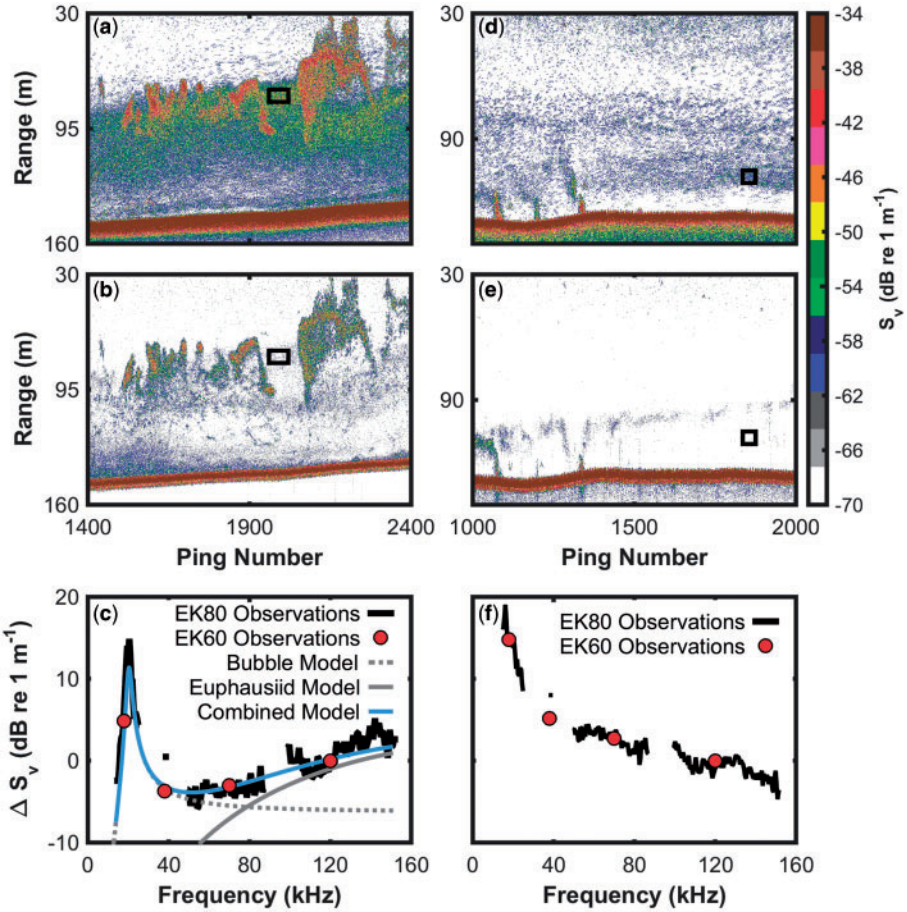

Figure 7. Examples where broadband frequency responses provide addition information compared with narrowband measurements. (a-b) Broadband echograms (a—18 kHz; b—120 kHz) of a walleye pollock aggregation and other, unknown scatterers. The boxes highlight the area used to produce the frequency response shown in (c) for the unknown near-resonant scatterers surrounding the aggregation. (c) ΔS_v spectrum for the area highlighted in (a) and (b) whose spectrum suggests the presence of small fish and euphausiids. A resonance peak is evident at 20.5 kHz while at higher frequencies the spectrum is consistent with euphausiids. The combined model curve is the incoherent addition of the resonance and euphausiid scattering curves. Narrowband observations agree well with broadband data but do not capture the resonance peak. (d-e) Broadband echograms (d—18 kHz; e—120 kHz) of a rockfish aggregations with other, unknown scatterers throughout the water column. (f) ΔS_v spectrum for the area highlighted in (d) and (e). The slope at the lowest frequencies suggests near-resonance scattering.

Likewise, volume backscatter spectra can vary widely for an individual species within a single school and between aggregations. Variability in the frequency response for individual aggregations is a major challenge relating to species discrimination. Averaging is necessary to produce smooth curves that can be applied in spectrally-based discrimination algorithms with high levels of statistical confidence. Effective use of ΔS_v curves as a criterion in species discrimination requires that differences among species are consistently observed not only when averaged over many aggregations, but also the scales over which the classification will be made *in situ*. Where the frequency response does not capture a defining feature of the scattering associated with the particular species (e.g. swimbladder resonance or the transition between scattering regimes for fluid-like scatterers), structural similarities to spectra from other species are likely. Here, all of the swimbladder-bearing fish species, with the exception of the mesopelagic fishes, were observed above swimbladder resonance.

This study, as well as historical observations (De Robertis *et al.*, 2010), indicate that the variability in ΔS_v spectra at a given frequency, both from within a single aggregation or separate aggregations, can be equal to or greater than the expected differences among species. Although differences in morphology may cause marginally different scattering spectra when they are highly averaged or observed in a well-controlled environment (e.g. Conti and Demer, 2003), in practice, these differences may be masked by the high degree of variability in field measurements. As a result, discrimination techniques based on ΔS_v and the slope of ΔS_v are unlikely to produce statistically meaningful results for single pings except in the most obvious cases (e.g. euphausiids vs. swimbladder-bearing fish). These challenges also extend to aggregations. For example, in addition to overlapping ΔS_v distributions, the observed slopes of ΔS_v for individual, single-species aggregations of walleye pollock and Pacific ocean perch were similar. The mean observed slope for walleye pollock aggregations is −1.4 dB/100 kHz (range: −3.5 to −0.1 dB/100 kHz) vs. −1.8 dB/100 kHz (range: −2.7 to −0.5 dB/100 kHz) for Pacific ocean perch. As a result, one could not confidently assign backscatter to walleye pollock vs. Pacific ocean perch based on these metrics alone and the same

conclusion likely applies to other acoustically similar species. The single capelin and herring aggregation, a diffuse layer, did have a steeper frequency response than the other fishes, as previously reported for capelin (De Robertis *et al.*, 2010). Unfortunately, with only one aggregation, there were not sufficient data to determine whether this difference is consistently observed.

Despite these challenges, there are situations in which broadband measurements at frequencies commonly used in fisheries acoustics provide valuable information to help discriminate among biological sources of scattering. Although flesh, organs, and bones contribute to backscattering from all fishes, the backscattering cross section of swimbladder-bearing fishes is dominated by the gas inclusion (Foote, 1980). Variations in target strength or volume backscatter as a function of frequency that are attributed to morphological differences between fishes lacking swimbladders have been previously identified (Gorska *et al.*, 2007; Johnsen *et al.*, 2009; Korneliussen, 2010; Jech *et al.*, 2017), and could be more effectively exploited with nearly continuous spectra. Another example is scattering at or near resonance (Verma *et al.*, 2017), when the peak can, with some assumptions, provide an indication of the size of the gas inclusion or swimbladder (Love, 1978; Benfield *et al.*, 2003). The additional frequency content of broadband signals can also be helpful in the case of mixed-species aggregations when it can help differentiate between dominant scattering sources in different portions of the spectra (Figure 7). Likewise, the dominant size of animals in zooplankton aggregations can be better constrained by nearly continuous S_v spectra curves if the transition between scattering regimes associated with the size of the animals is observed (Greenlaw, 1979; Holliday and Pieper, 1995; Lavery *et al.*, 2007). The improved range resolution and additional frequency content may also allow for better resolution of morphological features of targets that could be exploited for species discrimination (Stanton *et al.*, 2003; Reeder *et al.*, 2004; Lee *et al.*, 2012).

Elevated levels of backscatter in the 18 and 38 kHz channels in this study that suggested resonance or near-resonance scattering was observed in many locations. Improvements in operational capacity between 25 and 50 kHz would likely reveal benefits not fully realized in this work due to a combination of factors that limited the broadband operation of the system in this frequency range. First, this work used the Simrad ES38B transducer, which is not designed for broadband operation. New 38 kHz transducers designed for operation over a wider bandwidth will help overcome this limitation. High noise levels throughout the cruise motivated a post-cruise investigation into the source of the decreased signal-to-noise ratios when compared with previous surveys. These noise levels were later attributed to a salt water intrusion into the cable. Finally, hardware limitations at the time of the study limited the 38 kHz channel to operation using the "slow" taper, which results in decreased signal-to-noise ratios where the bandwidth is suppressed (Demer *et al.*, 2017; Lavery *et al.*, 2017). Given that these factors should not constrain future studies, studies of mesopelagic fishes and other organisms with peaks in backscatter between 25 and 50 kHz will likely benefit from the use of broadband systems.

The application of broadband scattering techniques at lower frequencies ($f < 10$ kHz) to exploit swimbladder resonance may also improve species or size class discrimination (Holliday, 1972; Jagannathan *et al.*, 2009; Gong *et al.*, 2010; Stanton *et al.*, 2010, 2012), thereby reducing a key source of uncertainty in abundance estimates derived from AT surveys (Woillez *et al.*, 2016). Despite some clear advantages, these lower-frequency approaches have the same complexities as other broadband techniques in addition to other technical and operational challenges related to noise, the transducer size, calibration procedures, and environmental concerns related to the use of low- to mid-frequency active sonars.

A number of challenges and uncertainties related to the use of broadband echosounders were not directly addressed in this manuscript. First, precise calibration techniques and processing parameters for calibration should be further refined for adaptation in survey applications. Standardized methodology should be developed for calculating spectra to limit the introduction of calibration artefacts, which can become apparent in post-processing when calculating highly averaged target strength or volume backscatter curves. Examples of one such artefact appear in the curves in Figure 6 (the local maximum between 120 and 140 kHz), where most of the curves contain similar frequency responses. These artefacts could have been manually removed, but were instead retained to highlight their impact and the need for procedures to deal with this challenge.

Broadband data can be processed using a range of window sizes. A longer data window means more data are captured and the resulting spectrum will have higher frequency resolution. A window as short as a few centimetres may adequately capture the target strength of a point scatterer or an individual fish (Demer *et al.*, 2017), whereas a longer window may be desired for analysis of fish schools. Acoustic features captured in the temporal domain manifest themselves in the frequency domain and processing windows should be chosen to match the application. Future work should identify optimal processing parameters for different applications. In some applications, rather than creating nearly continuous spectra, band-averaging over a specified bandwidth to produce curves more similar to narrowband observations, but with more data points, may prove to be a practical solution. Finally, observations in this study used synchronous pinging during calibration and broadband transects. This approach may be susceptible to cross-talk between the channels even without overlapping bandwidths (Demer *et al.*, 2017). Future studies should consider the implications of synchronous operation in field applications.

Conclusions

Species discrimination using broadband scattering techniques faces the same challenges as narrowband approaches at similar frequencies. Discrimination among acoustically similar taxa remains a challenge because of the variability observed *in situ* and the limitations of the scattering physics. For example, measurements of swimbladder-bearing fishes including walleye pollock, Pacific ocean perch, and Pacific herring resulted in similar broadband frequency responses. Furthermore, basic frequency differencing and slope-fitting algorithms are unlikely to greatly improve the discriminatory power of broadband measurements. Nonetheless, examples demonstrating the benefits of broadband operation that identified peaks in acoustic scattering that could be missed with narrowband measurements highlight the potential of the technology in other applications. The challenges of working with broadband systems will be reduced as the technology is more widely adopted and new processing techniques are developed to identify and exploit the additional information inherent in broadband signals. This streamlining of the processing may facilitate the analysis of larger datasets and the development of more effective species discrimination algorithms. Until these algorithms and processing techniques are optimized for the application and provide near real-time information, it seems likely

that routine abundance surveys will continue to rely on narrowband measurements.

Supplementary data

Supplementary material is available at the *ICESJMS* online version of the article.

Acknowledgements

The authors would like to thank Tom Weber for participating in the survey and providing WBTs. The following Alaska Fisheries Science Centre staff provided operational support: Scott Furnish, Darin Jones, Taina Honkalehto, Patrick Ressler, Denise McKelvey, Robert Levine, Nate Lauffenburger, and Emily Collins. We also acknowledge three NOAA Teachers at Sea (Vincent Colombo, Nicholette Durkan, and Andrea Schmuttermair) for their help processing the trawl-haul catch. We acknowledge the contributions of the crew of the NOAA Ship *Oscar Dyson*. Without the generous equipment loans from Simrad this work would not have been possible. Two anonymous reviewers provided valuable feedback on the draft manuscript. This work was supported by funding from NOAA's Office of Science and Technology, Advanced Sampling Technology Working Group. Reference to trade names does not imply endorsement by the National Marine Fisheries Service, NOAA.

References

Atkins, P., Francis, D. T., and Foote, K. G. 2008. Calibration of broadband sonars using multiple standard targets. Proceedings of the Ninth European Conference on Underwater Acoustics, 1: 261–266.

Benfield, M. C., Lavery, A. C., Wiebe, P. H., Greene, C. H., Stanton, T. K., and Copley, N. J. 2003. Distributions of physonect siphonulae in the Gulf of Maine and their potential as important sources of acoustic scattering. Canadian Journal of Fisheries and Aquatic Sciences, 60: 759–772.

Chapman, R. P., and Marshall, J. R. 1966. Reverberation from deep scattering layers in the North Atlantic. Journal of the Acoustical Society of America, 40: 405–411.

Chu, D., and Stanton, T. K. 1998. Application of pulse compression techniques to broadband acoustic scattering by live individual zooplankton. Journal of the Acoustical Society of America, 104: 39–55.

Conti, S. G., and Demer, D. A. 2003. Wide-bandwidth acoustical characterization of anchovy and sardine from reverberation measurements in an echoic tank. ICES Journal of Marine Science, 60: 617–624.

Coyle, K. O., and Pinchuck, A. I. 2002. The abundance and distribution of euphausiids and zero-age pollock in the inner shelf of the southeast Bering Sea near the Inner Front in 1997-1999. Deep-Sea Research II, 49: 6009–6030.

De Robertis, A., McKelvey, D., and Ressler, P. H. 2010. Development and application of empirical multi-frequency methods for backscatter classification. Canadian Journal of Fisheries and Aquatic Sciences, 67: 1459–1474.

Demer, D. A., Andersen, L. N., Bassett, C., Berger, L., Chu, D., Condiotty, J., Cutter, G. R. *et al.* 2017. 2016 USA–Norway EK80 Workshop Report: Evaluation of a wideband echosounder for fisheries and marine ecosystem science. ICES Cooperative Research Report No. 336. 69 pp.

Demer, D. A., Berger, L., Bernasconi, M., Bethke, E., Boswell, K., Chu, D., Domokos, R. *et al.* 2015. Calibration of acoustic instruments. ICES Cooperative Research Report No. 326. 130 pp.

Dougherty, A. B., Bailey, K. M., and Mier, K. L. 2007. Interannual differences in growth and hatch date distributions of age-0 year walleye pollock Theragra chalcogramma (Pallas) sampled from the Shumagin Islands region of the Gulf of Alaska, 1985–2001. Journal of Fish Biology, 71: 2007.

Dragonette, L. R., Numrich, S. K., and Frank, L. J. 1981. Calibration Technique for acoustic scattering measurements. Journal of the Acoustic Society of America, 69: 1186–1189.

Ehrenberg, J. E., and Torkelson, T. C. 2000. FM slide (chirp) signals: a technique for significantly improving the signal-to-noise performance in hydroacoustic assessment systems. Fish Research, 47: 193–199.

Fernandes, P. G. 2009. Classification trees for species identification of fish-school echotraces. ICES Journal of Marine Science, 66: 1073–1080.

Foote, K. G. 1980. Importance of the swimbladder in acoustic scattering of fish: a comparison of gadoid and mackerel target strengths. Journal of the Acoustic Society of America, 67: 2084–2089.

Foote, K. G. 2000. Standard-target calibration of broadband sonars. Journal of the Acoustic Society of America, 108: 2484.

Foote, K. G., and MacLennan, D. N. 1984. Comparisons of copper and tungsten carbide calibration spheres. Journal of the Acoustic Society of America, 75: 612–616.

Francois, R. E., and Garrison, G. R. 1982a. Sound absorption based on ocean measurements: Part I: pure water and magnesium sulfate contributions. Journal of the Acoustic Society of America, 72: 896–907.

Francois, R. E., and Garrison, G. R. 1982b. Sound absorption based on ocean measurements: Part II: boric acid contribution and equation for total absorption. Journal of the Acoustic Society of America, 72: 1879–1890.

Gong, Z., Andrews, M., Jagannathan, S., Patel, R., Jech, J. M., Makris, N., and Ratilal, P. 2010. Low-frequency target strength and abundance of shoaling Atlantic herring (Clupea harengus) in the Gulf of Maine during the Ocean Acoustic Waveguide Remote Sensing 2006 Experiment. Journal of the Acoustic Society of America, 127: 104–123.

Gorska, N., Korneliussen, R. J., and Ona, E. 2007. Acoustic backscatter by schools of adult Atlantic mackerel. ICES Journal of Marine Science, 64: 1145–1151.

Greenlaw, C. F. 1979. Acoustical estimation of zooplankton populations. Limnology and Oceanography, 24: 226–242.

Guttormsen, M. A., McCarthy, A., and Jones, D. T. 2010. Results of the February-March 2009 echo integration-trawl surveys of walleye pollock (*Theragra chalcogramma*) conducted in the Gulf of Alaska, Cruises DY2009-01 and DY2009-04. AFSC Processed Report 2010-01, 67 p. Alaska Fish. Sci. Cent., NOAA, Natl. Mar. Fish. Serv., 7600 Sand Point Way NE, Seattle WA 98115.

Henkart, P. 2006. Chirp sub-buttom profiler processing - a review. Sea Technology, 35–38.

Hobæk, H., and Forland, T. N. 2013. Characterization of target spheres for broad-band calibration of acoustic systems. Acta Acustica united with Acustica, 99: 465–476.

Holliday, D. V. 1972. Resonance structure in echoes from schooled pelagic fish. Journal of the Acoustic Society of America, 51: 1322–1332.

Holliday, D. V., and Pieper, R. E. 1995. Bioacoustical oceanography at high frequencies. ICES Journal of Marine Science, 52: 279–296.

Horne, J. K. 2000. Acoustic approaches to remote species identification: a review. Fisheries Oceanography, 9: 356–371.

Jagannathan, S., Bertsatos, I., Symonds, D., Chen, T., Nia, H. T., Jain, A. D., Andrews, M., *et al.* 2009. Ocean Acoustic Waveguide Remote Sensing (OAWRS) of marine ecosystems. Marine Ecology Progress Series, 395: 137–160.

Jech, J. M., Lawson, G. L., and Lavery, A. C. 2017. Wideband acoustic volume backscattering spectra (15-260 kHz) of northern krill (Meganyctiphanes norvegica) and butterfish (Peprilus triacanthus). ICES Journal of Marine Science, 74: 2249–2261.

Jech, J. M., and Michaels, W. L. 2006. A multifrequency method to classify and evaluate fisheries acoustics data. Canadian Journal of Fisheries and Aquatic Sciences, 63: 2225–2235.

Johnsen, E., Pedersen, R., and Ona, E. 2009. Size-dependent frequency response of sandeel schools. ICES Journal of Marine Science, 66: 1100–1105.

Jones, D. T., Stienessen, S. C. and Lauffenburger, N., 2017. Results of the acoustic trawl survey of walleye pollock (Gadus chalcogrammus) in the Gulf of Alaska, June-August 2015 (DY2015-06). AFSC Processed Rep. 2017-03, 102 p. Alaska Fish. Sci. Cent., NOAA, Natl. Mar. Fish. Serv., 7600 Sand Point Way NE, Seattle WA 98115.

Korneliussen, R. J. 2010. The acoustic identification of Atlantic mackerel. ICES Journal of Marine Science, 67: 1749–1758.

Korneliussen, R. J., Heggelund, Y., Eliassen, I. K., and Johansen, G. O. 2009. Acoustic species identification of schooling fish. ICES Journal of Marine Science, 66: 1111–1118.

Korneliussen, R. J., Heggelund, Y., Macaulay, G. J., Patel, D., Johnsen, E., and Eliassen, I. K. 2016. Acoustic identification of marine species using a feature library. Methods in Oceanography, 17: 187–205.

Korneliussen, R. J., and Ona, E. 2003. Synthetic echograms generated from the relative frequency response. ICES Journal of Marine Science, 60: 636–640.

Lavery, A. C., Bassett, C., Lawson, G. L., and Jech, J. M. 2017. Exploiting signal processing approaches for broadband echosounders. ICES Journal of Marine Science, 74: 2262–2275.

Lavery, A. C., Chu, D., and Moum, J. 2010. Measurements of acoustic scattering from zooplankton and oceanic microstructure using a broadband echosounder. ICES Journal of Marine Science, 67: 379–394.

Lavery, A. C., Geyer, W. R., and Scully, M. E. 2013. Broadband acoustic quantification of stratified turbulence. Journal of the Acoustic Society of America, 134: 40–54.

Lavery, A. C., Wiebe, P. H., Stanton, T. K., Lawson, G. L., Benfield, M. C., and Copley, N. 2007. Determining dominant scatterers of sound in mixed zooplankton populations. Journal of the Acoustic Society of America, 122: 3304–3326.

Lee, W., Lavery, A. C., and Stanton, T. K. 2012. Orientation dependence of broadband acoustic backscattering from live squid. Journal of the Acoustic Society of America, 131: 4461–4475.

Love, R. H. 1978. Resonance acoustic scattering by swimbladder-bearing fish. Journal of the Acoustic Society of America, 64: 571–580.

McClatchie, S., Thorne, R. E., Grimes, P., and Hanchet, S. 2000. Ground truth and target identification for fisheries acoustics. Fisheries Research, 47: 173–191.

Medwin, H., and Clay, C. S. 1998. Fundamentals of Acoustical Oceanography. Boston, Academic Press.

Methot, R. D. 1986. Frame trawl for sampling pelagic juvenile fish. CalCOFI Report, XXVII: 267–278.

Papadakis, E. P., and Fowler, K. A. 1969. Broad-band transducers: radiation field and selected applications. Journal of the Acoustic Society of America, 50: 729–745.

Reeder, D. B., Jech, J. M., and Stanton, T. K. 2004. Broadband acoustic backscatter and high-resolution morphology of fish: Measurement and modeling. Journal of the Acoustic Society of America, 116: 747–761.

Ressler, P. H., De Robertis, A., Warren, J. D., Smith, J. D., and Kotwicki, S. 2012. Developing an acoustic index of euphausiid abundance to understand trophic interactions in the Bering Sea ecosystem. Deep-Sea Research II, 65–70: 184–195.

Ross, T., Keister, J. E., and Lara-Lopez, A. 2013. On the use of high-frequency broadband sonar to classify biological scattering layers from a cabled observatory in Saanich Inlet, British Columbia. Methods in Oceanography, 5: 19–38.

SIMFAMI. 2005. Species identification methods from acoustic multi-frequency information. Final report: Contract number Q5RS-2001-02054 486 pp.

Simmonds, E. J., and Armstrong, F. 1990. A wideband echo sounder: measurements of cod, saithe and herring, and mackerel from 28 to 54 kHz. Rapp. P.-v. Réun. Cons, int. Explor. Mer, 189: 381–387.

Simmonds, E. J., and MacLennan, D. N. 2005. Fisheries acoustics, 2nd. edn. Blackwell Science LTD, Oxford, UK 437 p.

Simonsen, K. A., Ressler, P. H., Rooper, C. N., and Zador, S. G. 2016. Spatio-temporal distribution of euphausiids: an important component to understanding ecosystem processes in the Gulf of Alaska and eastern Bering Sea. ICES Journal of Marine Science, 73: 2020–2036.

Smith, J. N., Ressler, P. H., and Warren, J. D. 2013. A distorted wave Born approximation target strength model for Bering Sea euphausiids. ICES Journal of Marine Science, 70: 204–214.

Stanton, T. K. 1989. Sound scattering by cylinders of finite length. III. Deformed cylinders. Journal of the Acoustic Society of America, 86: 691–705.

Stanton, T. K. 2012. 30 years of advances in active bioacoustics: a personal perspective. Methods in Oceanography, 1–2: 49–77.

Stanton, T. K., Chu, D., Jech, J. M., and Irish, J. D. 2010. New broadband methods for resonance classification and high-resolution imagery of fish with swimbladders using a modified commercial broadband echosounder. ICES Journal of Marine Science, 67: 365–378.

Stanton, T. K., Chu, D., Wiebe, P. H., Martin, L., and Eastwood, R. L. 1998. Sound scattering by several zooplankton groups I: experimental determiniation of dominant scattering mechanisms. Journal of the Acoustic Society of America, 103: 225–235.

Stanton, T. K., Reeder, D. B., and Jech, J. M. 2003. Inferring fish orientation from broadband-acoustic echoes. ICES Journal of Marine Science, 60: 524–531.

Stanton, T. K., Sellers, C. J., and Jech, J. M. 2012. Resonance classification of mixed assemblages of fish with swimbladders using a modified commercial broadband acoustic echosounder at 1-6 kHz. Canadian Journal of Fisheries and Aquatic Sciences, 69: 854–868.

Stauffer, G. C. 2004. NOAA Protocols for Groundfish Bottom Trawl Surveys of the Nation's Fishery Resources, U.S. Department of Commerce. NOAA Technical Memorandam. NMFS-F/SPO-65: 205 p.

Turin, G. L. 1960. An introduction to matched filters. IRE Transactions on Information Theory, 6: 311–329.

Verma, A., Kloser, R. J., and Duncan, A. J. 2017. Potential use of broadband acoustic methods for micronekton classification. Acoustics Australia, doi:10.1007/s40857-017-0105-8.

Westerfield, E., Prager, R., and Stewart, J. 1960. Processing gains against reverberation (clutter) using matched filters. IEEE Transactions on Information Theory, 6: 342–348.

Wileman, D. A., Ferro R. S. T., Fonteyen R. and Millar R. B., (Eds), 1996. Manual of methods of measuring the selectivity of towed fishing gears. ICES Cooperative Research Report. 215, 126 pp.

Williams, K., Punt, A. E., Wilson, C. D., and Horne, J. K. 2011. Length-selective retention of walleye pollock, Theragra chalcogramma, by midwater trawls. ICES Journal of Marine Science, 68: 119–129.

Williams, K., Towler, R., and Wilson, C. 2010. Cam-Trawl: a combination trawl and stereo-camera system. Sea Technology, 51: 45–50.

Woillez, M., Ressler, P. H., Wilson, C. D., and Horne, J. K. 2012. Multifrequency species classification of acoustic-trawl survey data using semi-supervised learning with class discovery. Journal of the Acoustic Society of America, 131: EL184–EL190.

Woillez, M., Walline, P. D., Ianelli, J. N., Dorn, M. W., Wilson, C. D., and Punt, A. E. 2016. Evaluating total uncertainty for biomass- and abundance-at-age estimates from eastern Bering Sea walleye pollock acoustic-trawl surveys. ICES Journal of Marine Science, 73: 2208–2226.

Zakharia, M. E., Magand, F., Hetroit, F., and Diner, N. 1996. Wideband sounder for fish species identification at sea. ICES Journal of Marine Sciences, 53: 203–208.

Handling editor: Purnima Ratilal